European Journal of Neuroscience, Vol. 6, pp. 1619–1632, 1994

Relationship Between Lateral Inhibitory Connections and the Topography of the Orientation Map in Cat Visual Cortex

Zoltán F. Kisvárday, Dae-Shik Kim[1], Ulf T. Eysel and Tobias Bonhoeffer[1,2]
Ruhr-University Bochum, Department of Neurophysiology, Universitätsstrasse 150, MA 4/149, 44801 Bochum, Germany
[1]Max Planck Institute for Brain Research, Deutschordenstrasse 46, 60528 Frankfurt, Germany
[2]Max Planck Institute for Psychiatry, Am Klopferspitz 18A, 82152 München-Martinsried, Germany

Key words: visual cortex, optical recording, single cell reconstruction, basket cells, orientation selectivity

Abstract

The functional and structural topography of lateral inhibitory connections was investigated in visual cortical area 18 using a combination of optical imaging and anatomical tracing techniques in the same tissue. Orientation maps were obtained by recording intrinsic signals in regions of 8.4–19 mm^2. To reveal the inhibitory connections provided by large basket cells, biocytin was iontophoretically injected at identified orientation sites guided by the pattern of surface blood vessels. The axonal and dendritic fields of two retrogradely labelled large basket cells were reconstructed in layer III. Their axonal fields extended up to 1360 μm from the parent somata. In addition to single basket cells, the population of labelled basket cell axons was also studied. For this analysis anterogradely labelled basket axons running horizontally over 460–1280 μm from the core of an injection site in layer III were taken into account. The distribution of large basket cell terminals according to orientation preferences of their target regions was quantitatively assessed. Using the same spatial resolution as the orientation map, a frequency distribution of basket cell terminals dependent on orientation specificity could be derived. For individual basket cells, the results showed that, on average, 43% of the terminals provided input to sites showing similar orientation preferences (±30°) to those of the parent somata. About 35% of the terminals were directed to sites representing oblique-orientation [±(30–60)°], and 22% of them terminated at cross-orientation sites [±(60–90)°]. Furthermore, the possible impact of large basket cells on target cells at different distances and orientation preferences was estimated by comparing the occurrence of orientation preferences with the occurrence of basket terminals on the distance scale. It was found that a basket cell could elicit iso-orientation inhibition with a high impact between 100–400 and 800–1200 μm, strong cross-orientation inhibition at ~400–800 μm, and oblique-orientation inhibition between 300–500 and 700–900 μm from the parent soma. The non-isotropic topography of large basket axons suggests a complex function for this cell class, possibly including inhibition related to orientation and direction selectivity depending on the location of the target cells and possible target selectivity.

Introduction

A prominent feature of visual cortical neurons is that they are selective for oriented visual stimuli; an optimally oriented white or dark bar presented over the cell's receptive field elicits vigorous responses while a non-optimally oriented bar is less or not at all effective (Hubel and Wiesel, 1962). Although numerous studies have been carried out to unravel the mechanisms underlying orientation selectivity, this question is still unresolved. In the original excitatory model, Hubel and Wiesel (1962) proposed that orientation selectivity was acquired by the appropriate alignment of thalamic input fibres. Although this concept has recently got considerable support (Chapman *et al.*, 1991), it has been challenged by a number of physiological (Benevento *et al.*, 1972; Blakemore and Tobin, 1972; Creutzfeldt *et al.*, 1974; Henry *et al.*, 1974; Morrone *et al.*, 1982; Ramoa *et al.*, 1986) and combined pharmacological (Sillito, 1975, 1979; Tsumoto *et al.*, 1979; Eysel *et al.*, 1988, 1990; Crook and Eysel, 1992) experiments indicating the involvement of intracortical inhibitory mechanisms in direction and orientation selectivity. In the latter respect, the simplest idea was that non-optimally oriented stimuli activated neighbouring 'cross-oriented' GABAergic cells, which in turn directly inhibited the recorded cell (cross-orientation model). Consequently the type of GABAergic cell involved in such a mechanism should supply a powerful input to cross-orientation sites with respect to its own orientation preference. From the horizontal topography of orientation columns (Hubel and Wiesel, 1963, 1965; Albus, 1975; Cynader *et al.*, 1987; Bonhoeffer and Grinvald, 1991), one can conclude that this type of inhibitory cell should be capable

Correspondence to: Zoltán F. Kisvárday, as above

Received 2 March 1994, revised 11 May 1994, accepted 17 May 1994

of providing connections over at least 500–600 μm from the parent soma. At present the only candidate that could fulfil this structural–functional requirement is the so-called large basket cell, whose anatomical constraints are well suited for such a task (for review see Kisvárday, 1992). This was directly tested in a recent study, using a combination of electrophysiological mapping of orientation selectivity and labelling of layer III large basket cells with the tracer biocytin in the same tissue (Kisvárday and Eysel, 1993). It was observed that the axonal terminals of the same large basket cell often arborized at cross-orientation sites. However, the situation concerning the projection pattern of large basket cell axons to known orientation sites turned out to be more complex; using a semiquantitative assessment, the same study showed that the axonal terminals were encountered roughly in equal numbers at iso-, oblique- and cross-orientation sites, indicating that long-range lateral inhibition is associated not only with cross-orientation inhibition but also with iso-orientation inhibition involved in possibly direction-specific inhibition. Due to the limitation of the applied technique (limited number of electrode penetrations), however, the global topographic relationship between the basket axons and the distribution of orientation columns could not be disclosed. Therefore, in the present study we examine the functional topography of morphologically characterized large basket cells in direct comparison with the high-resolution topography of orientation selectivity obtained with the optical imaging technique. The results confirm our previous conclusion on the broad orientation range of sites targeted by lateral inhibitory connections. In addition to a more accurate assessment of their contribution to iso-, oblique- and cross-orientation sites, the topography of their targets as a function of lateral distance along the plane of the orientation map could be determined.

Some of these findings have been published in abstract form (Kisvárday *et al.*, 1992).

Materials and methods

Preparation and surgical procedures

Two adult cats were used in the present study. Anaesthesia was induced with ketamine hydrochloride (10–20 mg/kg, i.m.), supplemented in some cases by xylazine hydrochloride (2.5 mg/kg, i.m.) and maintained throughout the experiments using halothane/N_2O anaesthesia (70% N_2O/30% O_2 with 0.2–2% halothane). For muscle relaxation succinylcholine hydrochloride or hexacarbacholine bromide was administered intra-arterially at a rate of 20 or 0.3–1 mg/kg/h, respectively. End-tidal CO_2 (3–4%), EEG, ECG and body temperature (38°C) were continuously monitored. In both hemispheres, a craniotomy was performed at Horsley–Clarke co-ordinates A2. For reducing brain movement, a circular stainless steel chamber 22 mm in diameter was placed over the exposed region and mounted with dental cement (Paladur, Kulzer, Wehrheim, Germany) onto the skull. After removing the dura, the chamber was filled with silicone oil and sealed with a round glass coverslip.

Optical imaging

In general, optical recording provides a fast way of obtaining information about the distribution of orientation preferences over large regions. Nonetheless, it should be kept in mind that this technique detects signals arriving only from the superficial 600–900 μm of tissue, i.e. the supragranular layers of the cortex. Therefore any implication concerning deeper cortical structures has to be treated with caution. Further problems may arise from the fact that iso-orientation columns do not always run parallel to the optical axis of the imaging system. In particular, in convoluted regions this makes it difficult to extrapolate surface information on orientation preferences to deep structures. In order to reduce the number of possible errors we carried out our experiments in largely flat zones of area 18, where distortion in the organization of orientation columns due to geometrical perturbation was expected to be minimal. The surface of the cortex was illuminated by two adjustable light guides attached to a Zeiss tungsten–halogen lamp. The light was passed through interference filters of 605 ± 10 nm wavelength. A slow-scan CCD camera (Spektronics, Munich, Germany) was used for the imaging of intrinsic signals. Intrinsic imaging utilizes the fact that oxyhaemoglobin and deoxyhaemoglobin have very different absorption spectra (Frostig *et al.*, 1990). Therefore one can optically obtain a map of the tissue's metabolic demand for oxygen and hence a map of neuronal activity.

In order to present large-field visual stimuli to the animal a monitor was positioned at a distance of 30–45 cm so that in the properly refracted animal it stimulated an angle of 40–60° in the visual field, contralateral to the hemisphere investigated. A stimulating system developed by Kaare Christian (Rockefeller University, NY) was used to produce high-contrast square-wave gratings with a spatial frequency of 0.15 cycles/degree and a drift velocity of 15°/s on the stimulating screen. For functional imaging we normally presented a particular stimulus to both eyes of the cat for 3 s and recorded five frames of 600 ms duration with the CCD camera. This period of data acquisition was followed by a 7 s interstimulus interval after which the next stimulus was presented.

For data analysis we calculated 'single condition maps' (Bonhoeffer and Grinvald, 1993), which were the images acquired during a particular stimulus corrected for uneven illumination. 'Angle maps' (Blasdel and Salama, 1986; T'so *et al.*, 1990; Bonhoeffer and Grinvald, 1993) were computed to get a complete view of the organization of orientation preference in the investigated region of cortex. These maps (e.g. Fig. 6) present the preferred orientations for different cortical regions using a colour code.

Iontophoretic injection of biocytin

At the end of optical recordings, biocytin (2–5% in 0.5 M sodium acetate; Sigma, Deisenhofen, Germany) was iontophoretically delivered at one or multiple sites. In cat 1, four injections were placed in the same hemisphere (Fig. 1). In cat 2, one injection was made. All injections were aimed at particular locations with unambiguous orientation preference with the help of activity maps and corresponding vascular maps. Then the tracer-filled electrode was lowered with a manually controlled microdrive to a depth of 0.3–0.9 mm from the cortical surface. For iontophoretic delivery, positive current of 0.5–0.9 μA at 1 Hz with 0.5 s on/off duty cycle was applied for 20 min.

Since one of the main aims of this study was to analyse the relationship between the functional map and the underlying anatomical maps in the same tissue, it was essential to produce reference marks that allowed us to align the optical images with the histological sections. Therefore, in addition to the biocytin injections, 3–5 perpendicular electrode marks without iontophoretic delivery were made whose topographic locations were also registered on the vascular maps. The animals were allowed to survive 9–15 h. Finally, they were killed with a lethal dose of Nembutal and perfused transcardially with Tyrode's solution followed by fixative containing 2–4% paraformaldehyde (Merck, Darmstadt, Germany) and 0.5–2% glutaraldehyde (Merck, Darmstadt, Germany) in 0.1 M phosphate buffer (PB), pH 7.4.

Histological procedures

Large blocks of the area of interest were dissected. In order to preserve the three-dimensional distribution of biocytin-labelled elements

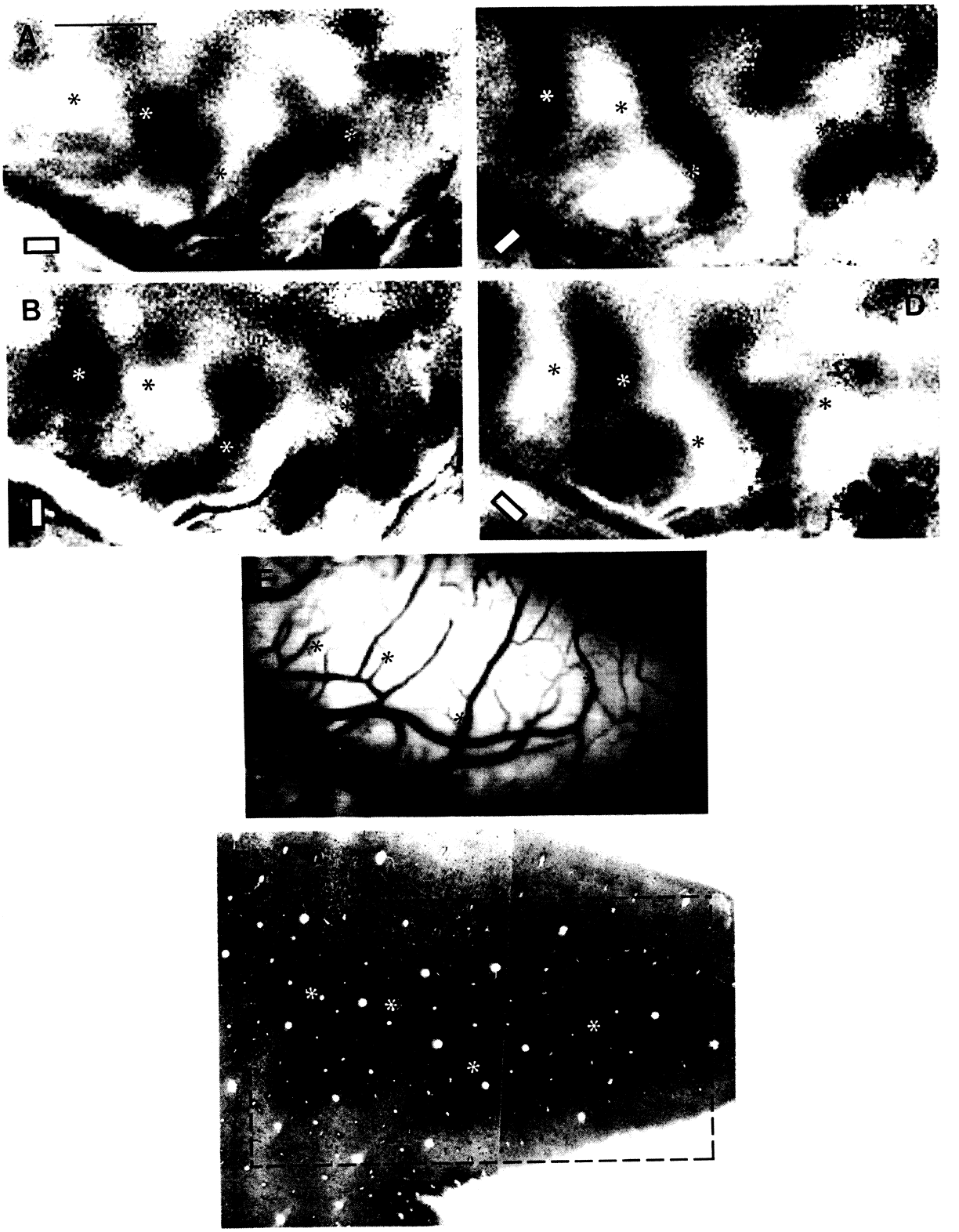

FIG. 1. (A–D) Optical activity images obtained in area 18 showing a region of 4.5×2.5 mm^2 of cortex. The dark regions represent highly active zones and the white regions represent the least active zones for the particular stimulus orientation shown in the lower left corner. In E, the vascular pattern of the same cortical region shown in A–D is visible. Asterisks indicate sites of iontophoretic injection of biocytin. After histological treatment, the four injection sites appear as dark spots in an 80 μm thick horizontal section taken from the same region. The framed area in F corresponds to the region subjected to optical recording. Bars: A–F, 1 mm.

flattening of the cortex was applied. Sections (70–80 μm thick) were cut on a vibratome in a plane parallel with the cortical surface and rinsed in PB with constant agitation in ten lots overnight. Biocytin labelling was revealed using avidin–biotin complexed with horseradish peroxidase (reagent ABC), as follows. The sections were washed in Tris-buffered saline containing 0.05% Triton X-100 (TBS-T, pH 7.6) for 3 × 20 min. Then the reagent ABC (1:200 in TBS-T, Vector, Laboratories, Burlingame, CA, USA) was applied overnight at 4°C. For the enzymatic reaction 0.05% 3,3′-diaminobenzidine-4HCl (DAB; Sigma, Deisenhofen, Germany) was used in Tris buffer (TB, pH 7.6) supplemented with 0.005% $CoCl_2$ intensification for 20 min. The reaction was completed by adding 10 μl of 1% H_2O_2 to every 2 ml of DAB solution. After thorough rinsing in 0.1 M TB followed by 0.1 M PB, the sections were treated in 1% OsO_4 (Sigma) in 0.1 M PB for 30 min, dehydrated, and embedded in Durcupan ACM (Fluka, Neu-Ulm, Germany) resin on slides.

Reconstruction of labelled basket cells

Labelled large basket cells were selected according to the completeness of their axonal arbors. Of 19 basket cells labelled around the five injection sites, two basket cells were chosen for detailed analysis in layer III (cells BC1 and BC2). The dendritic and axonal fields of each cell were pencil-drawn and reconstructed from 8–13 horizontal sections using a 50× oil objective and a microscope (Leitz Diaplan) fitted with a drawing tube. In addition, in cat 2, a population of basket axons that extended >400 μm laterally from the injection site were reconstructed in layer III. For aligning the labelled processes of neighbouring sections, corresponding cut ends of axons and landmarks, such as cross-sectionally running small blood vessels, were used.

Alignment of the optical images with the distribution of biocytin-labelled cells

A key issue of the present analysis is whether the physiological image of orientation preferences can be aligned with the anatomical images revealed with biocytin labelling. Therefore the plane of the optical images and the plane of histological sections were set as parallel with the cortical surface as possible. Another important factor that needs to be considered is tissue shrinkage caused by fixation and subsequent histological procedures; the stronger the tissue shrinkage the more severe is the mismatch between the physiological and the anatomical images. We utilized the mechanical damage caused by the glass electrode that was readily visible in the osmicated sections. Penetration marks including the injection site appeared as dark, slightly oedematous spots, often containing a few red blood cells and/or darkly stained macrophages under the light microscope (see Fig. 1A in Kisvárday and Eysel, 1993). They were reconstructed from consecutive sections using a similar procedure to that used for labelled cells (see above). The course of these electrode tracks could be traced up to the most superficial sections representing the entry of the electrode, and, according to this level, their topographic location could be determined. The relative position of the histologically reconstructed penetration marks and that of their aimed location on the physiological map matched with a ±(60–105) μm confidence range.

Finally, using the same penetration marks with known lateral distances we estimated the tissue shrinkage caused by perfusion and histological treatment: cat 1, 0.951; cat 2, 0.970. In the following, all numerical values and scale bars have been corrected by the individual shrinkage factor.

Resolution and error during histological reconstruction

Optical images were recorded with an image resolution between 28 × 23 and 50 × 50 μm^2 per pixel. For a direct comparison between such a fine image and the anatomical image one has to consider that the error made during any stage of histological reconstruction ought to be within the resolution range of the corresponding optical image. According to this directive we measured the maximal lateral displacement of corresponding branches of the reconstructed cells and that of penetration sites between adjacent sections and found that they had an overall horizontal error of ~20 and 30–40 μm respectively. Therefore the anatomical reconstruction contributed an error in the range of the optical image resolution. It thus seems likely that the alignment procedure actually depends upon the accuracy of guiding the electrodes into their aimed location. Finally, it is important that the overall error made during the alignment procedure remains in the range well below the size of an iso-orientation 'column', a so-called functional unit that is ~100–150 μm in diameter (Hubel and Wiesel, 1962; Albus, 1975). The accuracy of electrode positioning in relation to the orientation map (vascular map) can be estimated in the range of ±100 μm. Therefore, a direct analysis between the topography of orientation maps and the topography of the underlying inhibitory networks of large basket cells could be performed.

Cortical layers

The laminar location of labelled somata and axonal collaterals was determined on the basis of characteristic structural features such as neuron density, soma size, and the presence of layer-specific cell types, in particular large pyramidal cells at the border region of layers III and IV. The types of biocytin-labelled neurons, including those which were not subject of this study, were also indicators of laminar boundaries.

Quantitative analysis of labelling with respect to orientation maps

In order to study the possible physiological impact of labelled basket cells over the entire region of their axonal arborization, a direct comparison between their bouton distribution and the distribution of optically obtained orientation sites was conducted as follows. Using an appropriate shrinkage factor (see above), the boutons of each reconstructed basket cell were redrawn and the resulting bouton distributions were manually aligned and overlaid with a meshgrid of the same pixel size as that of the corresponding optical image. In this way the number of terminals falling within each pixel was determined and the resulting matrix was fed into an IBM-compatible personal computer. A frequency distribution of axonal terminals was then computed with respect to 16 orientation divisions, each of which represented a range of 11.25°, covering the whole range of orientations between 0° and 180°.

In a further approach, the 'relative impact' of basket cell terminals as a function of lateral distance from the parent soma and, in the case of the population of layer III basket axons, from the injection site was also estimated. Accordingly, each basket axon was overlaid with concentric rings of 100 μm width centred on the parent soma and the injection site. The number of terminals associated with the three different orientation preference ranges representing iso- (±30°), oblique- (±[30–60]°) and cross-orientation [±(60–90)°] was determined within each ring and expressed as a percentage of the total number of terminals.

Results

Orientation maps

In vivo optical imaging resulted in high-resolution functional maps showing orientation preferences over large regions of area 18. The patchy pattern of iso-orientation sites was consistent with previous

FIG. 2. Light microscopic characteristics of biocytin-labelled large layer III basket cells in an area that had been mapped for orientation with the optical imaging technique. In A, asterisks indicate the somata of reconstructed basket cells BC1 and BC2 in a horizontal section. One of the smooth dendrites of BC1 is labelled by arrowheads. BC1 and a labelled pyramidal cell in the framed area are also shown in B. Note the large soma size of the basket cell. In addition axonal terminals emitted by BC1 provide pericellular contacts (arrows) onto an unlabelled cell. C and D are typical examples of basket cell axons and terminals. In C, some of the boutons (arrowheads) surround the apical dendritic shaft (in the horizontal plane) of a pyramidal cell. Other terminals (arrows) form pericellular nests. In D, a myelinated main axon (arrowheads) emits short collaterals laden with boutons, some of which establish perisomatic contacts (arrows) onto other neurons. Bars: A, 50 μm; B–D, 10 μm.

results showing an average diameter of 400–600 μm (Bonhoeffer and Grinvald, 1991, 1993). It is noteworthy that some of the iso-orientation patches were slightly elongated, as shown in Figure 1. A particular pattern of iso-orientation domains was observed in animal 2, in which the orientation patches were aligned in rows running perpendicular to the border with area 17.

TABLE 1.

Cat	Basket cell	Layer	Number of terminals (B) and dendritic segments (D) at sites of							
			iso-orientation ±30		oblique-orientation ±(30–60)°		cross-orientation ±(60–90)°		total	
			B	D	B	D	B	D	B	D
1	BC1	III	1222 (44.4)	149 (74.5)	1047 (38/1)	39 (19.5)	482 (17.5)	12 (6.0)	2751 (100)	200 (100)
	BC2	III	492 (38.2)	164 (98.8)	375 (29.6)	2 (1.2)	401 (31.6)	0 (0.0)	1268 (100)	166 (100)
	Subtotal		1714 (42.6)	313 (85.5)	1422 (35.4)	41 (11.2)	883 (22.0)	12 (3.3)	4031 (100)	366 (100)
2	Pooled axons	III	811 (42.2)		424 (22.1)		688 (35.8)		1923 (100)	
	Total		2525 (42.5)		1846 (31.1)		1571 (26.4)		5942 (100)	

Numbers in parentheses are percentage values.

Injection sites

In cat 1, four injections were made in layers III/IV in the same hemisphere. Two large basket cells (BC1 and BC2) in layer III, whose axonal and dendritic fields lay chiefly outside the densely labelled zone, were reconstructed in serial sections. In cat 2, biocytin was injected at one location and the histological reconstruction showed that the relatively small injection produced mainly anterograde labelling of fibres. Only a few labelled somata were found around the injection site and they were weakly labelled.

Labelled basket cells

In each animal, the labelling was screened for the presence of large basket cell axons whose anatomical features could be readily distinguished from other types of cortical neurons. Briefly, the main axons along their course were heavily myelinated and ran horizontally over 1–1.5 mm from the parent soma (Fig. 2D). Characteristically they emitted secondary collaterals at quasi-regular intervals, which in turn gave off short radial segments studded with bulbous boutons impinging upon the perisomatic region of other cells (Fig. 2C, D). When such axons could be traced to their origin they always emerged from large, radially elongated somata of 20–35 μm diameter bearing beaded, spine-free dendrites (Fig. 2A, B). The dendritic field of these cells often reached 500–700 μm in diameter and was elongated along the course of apical dendrites (for review see Kisvárday, 1992).

Single basket cells

Two large basket cells were reconstructed whose somata and dendrites were strongly labelled in layer III (Figs 3 and 4). Their axonal fields were restricted to the same layer, though some of the terminal branches entered layers II and upper IV. The lateral extent of basket axons measured from the parent somata was 1.39 mm for BC1 and 1 mm for BC2. In this respect, however, it is conceivable that some of the axons entering the core of the injection sites could not be traced. Therefore, both the geometrical values and the bouton counts shown in Table 1 represent the lower estimate for these cells.

Population of basket axons

In addition to single cells contributing to lateral inhibition, we were interested to know how the population of large basket axons labelled from the same cortical column distributes over regions of known orientation preferences. Therefore, in animal 2 all labelled axons with the morphology of large basket cells and whose lateral extent exceeded 400 μm from the core of the injection site were reconstructed in layer III. A total of eight basket axons were found (Fig. 5). Like the axons of single basket cells described above, they occasionally entered neighbouring layers with more towards upper layer IV. An interesting feature of the resulting axonal field composed of many axons was that it occupied only certain wedge-shaped sectors along the plane parallel with the cortical surface. This phenomenon was very similar to the axonal field of single basket cells. Its territory was elongated in the antero-posterior direction, showing a maximum extent of 1.28 mm (Fig. 5).

A critical issue in the anlysis of the above axon population with regard to orientation was whether the parent somata of these axons were located within or outside the injection site. According to the first possibility, the pool of labelled axons represented the same orientation preferences as that of the injection site. In the second instance they represented a mixture of many different orientation preferences of a number of topographic locations. At this point there are two important observations to be mentioned. First, each reconstructed basket axon showed intense labelling. If these axons originated from outside the injection site then the parent somata would have shown intense labelling due to retrograde transport of the tracer. In fact such strongly labelled somata were not found. Secondly, some labelled dendrites at the injection site showed characteristics of non-pyramidal neurons, e.g. they were smooth and occasionally beaded. In the light of these arguments we concluded that the strongly labelled basket axons originated from a small number of basket cells, most likely 3–4, whose somata might have been hidden in the densely labelled core zone.

The distribution of basket cell input to sites of known orientation

Optical imaging of orientation preferences and biocytin labelling in the same tissue allowed us to carry out a direct analysis of the functional topography of large basket cells. Because signal transduction between neurons takes place at synaptic junctions, the functionally relevant output sites of a neuron can actually be associated with the location of its axonal terminals. Therefore, a quantitative estimate for the inhibitory contribution of basket axons was made by plotting the bouton distribution of reconstructed basket axons in alignment with

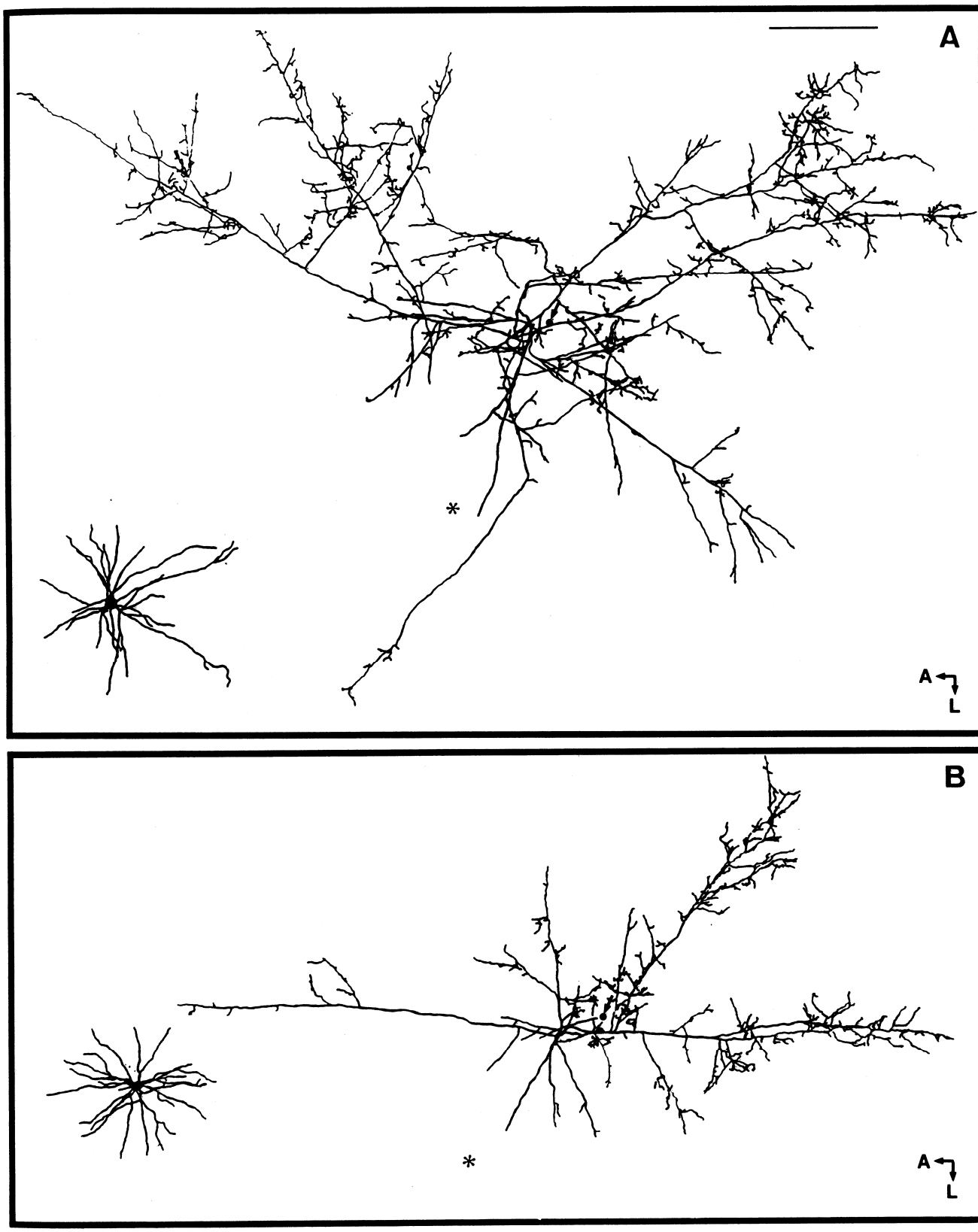

FIG. 3. Drawing of biocytin-labelled large basket cells BC1 (A) and BC2 (B) in a plane parallel to the cortical surface. The respective parent somata and dendritic fields of the two cells are shown in the lower left corners. Their locations are also indicated within the axonal fields (arrowed dots). The relative position of the injection site to the axonal fields is marked by an asterisk. A, anterior; L, lateral. Bar: A and B, 500 μm.

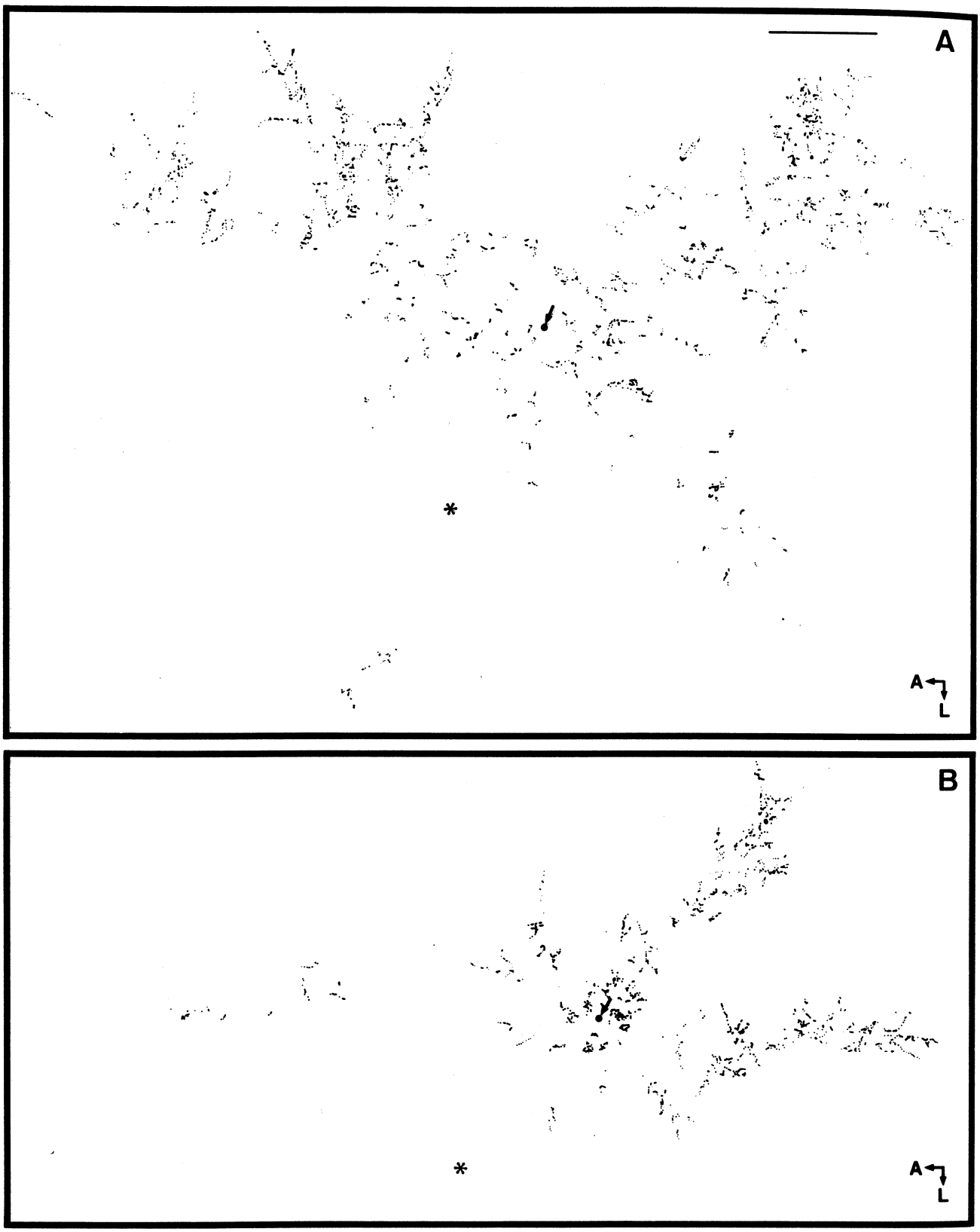

FIG. 4. Bouton distribution of basket cells BC1 (A) and BC2 (B) shown in Figures 3A and B, respectively. The parent somata are indicated by arrowed dots, and the injection site is labelled by an asterisk. A, anterior; L, lateral. Bar: A and B, 500 μm.

FIG. 5. Horizontal view of the axon (on the left) and bouton (on the right) distribution of eight basket cell collaterals radiating out from the injection site (asterisks) in layer III. Each basket collateral arborized in layers III and upper IV. A, anterior; L, lateral. Bar: 250 μm.

the orientation map of corresponding regions (see Materials and methods). At this point, it is important to note that none of the labelled basket cell somata and the injection site of cat 2 were confined to a so-called orientation centre (Bonhoeffer and Grinvald, 1991).

Single-cell analysis

In a first attempt to assess whether individual basket cells in layer III pick out sites of particular orientation to be engaged with or have no preference for special orientations, we qualitatively inspected the distribution of basket axons over orientation maps as shown for cell BC1 in Figure 6. It is obvious that this basket cell emits axonal branches to virtually all orientations represented by different colours. Even when single main axons of the same cell are examined, no selective accumulation of the collaterals (terminals) is apparent at any orientation. Rather the branches travel across many orientation

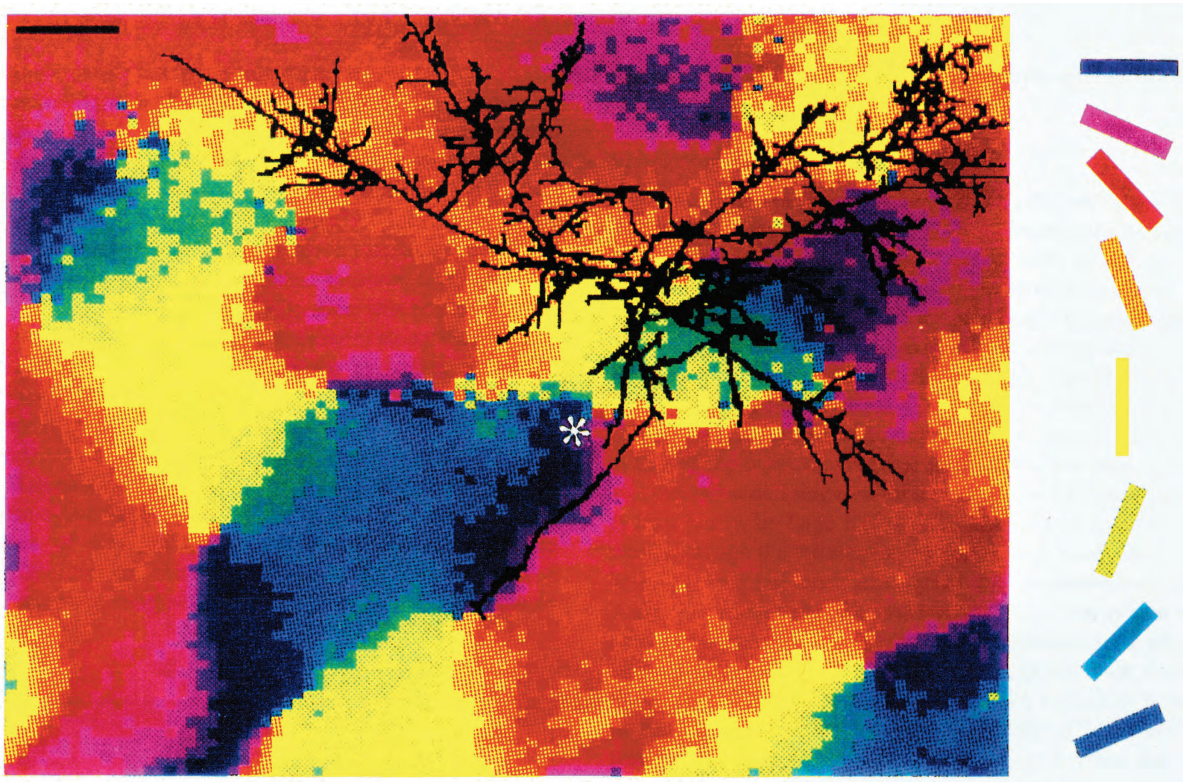

FIG. 6. Colour representation of orientation maps and the underlying distribution of basket axon BC1 (in black, also shown in Fig. 3A). For the sake of better visibility the axon is drawn thicker. The preferred orientation at each location (pixel) is coded according to the colour scheme shown on the right. Note that each axonal branch runs across regions representing many orientations. The injection site is marked by an asterisk. Bar: 250 μm.

preferences, often within short distances. In addition to these qualitative findings we carried out a quantitative analysis based on the assumption that the orientation preference of a basket cell resembles the orientation preference of other cells in its orientation column. According to this assumption the distribution of terminals of BC1 occupied regions representing the entire scale of orientation values, as demonstrated in Figure 7A. A similar broad distribution of terminals according to orientation was found for the other basket cell, BC2 (Fig. 7B). Interestingly, the axonal terminals of cell BC1, which had the most complete axonal arborization of the two basket cells, provided a skewed distribution (counter-clockwise) around the preferred orientation at the soma location (Fig. 7A). At present we do not know whether the skewed distribution of terminals corresponds to a genuine bias towards certain orientation preferences with respect to the cell's own orientation preference or whether it is the result of incomplete reconstruction due mainly to the fact that labelled axons at certain orientation sites, chiefly at the core of the injection site, could not be traced. A similar argument may apply for the dissimilarity between the two cells' bouton distribution according to orientation ranges. Obviously, these questions can only be resolved with certainty by intracellular labelling of large basket cells in combination with optical imaging. Importantly, however, our data showed that large basket cells could provide input to a broad range of orientations. In this respect we compared our data with previous results using a simple definition of iso-, oblique- and cross-orientation preferences for the targeted regions (Kisvárday and Eysel, 1993). Hence we dissected the optically imaged orientation maps according to zones representing iso- (±30°), oblique- [±(30–60)°] and cross-orientation [±(60–90)°] with respect to the basket cell's own orientation preference (Table 1). The results for the two basket cells showed that 42.6% of all terminals were directed to sites which represented iso-orientation preferences to that of the parent cells. Oblique- and cross-orientation sites were encountered by 35.4 and 22.0% of the terminals, respectively.

Population of axons in layer III

Without doubt the situation regarding the contribution of lateral inhibition from any given point in the visual cortex cannot be considered solely at the single-cell level. Therefore we studied what the population of basket cell axons do. The same method that was used to assess the distribution of single cell terminals at orientation sites was applied for the pooled axons in layers III. The result is shown in Figure 7C. We found that the distribution of axonal terminals according to orientation sites covered the entire scale of orientations; however, it was uneven in the sense that some orientations received more basket cell input than others.

Dendritic field of large basket cells

Another relevant question to be asked is whether the dendritic field of a large basket cell samples input from a similarly broad range of orientations to the orientation spectrum of its output site. Therefore we conducted a conservative analysis for the dendritic fields of basket cells BC1 and BC2. Accordingly, the number of dendritic segments running across each orientation pixel was counted and expressed proportional to iso-, oblique- and cross-orientation values. The results are shown in Table 1. Interestingly, in contrast to the axons, the dendrites were found to arborize in regions representing a relatively narrow range of orientations. On average, 86% of their branches occupied iso-orientation sites, ~11% of them crossed oblique-orienta-

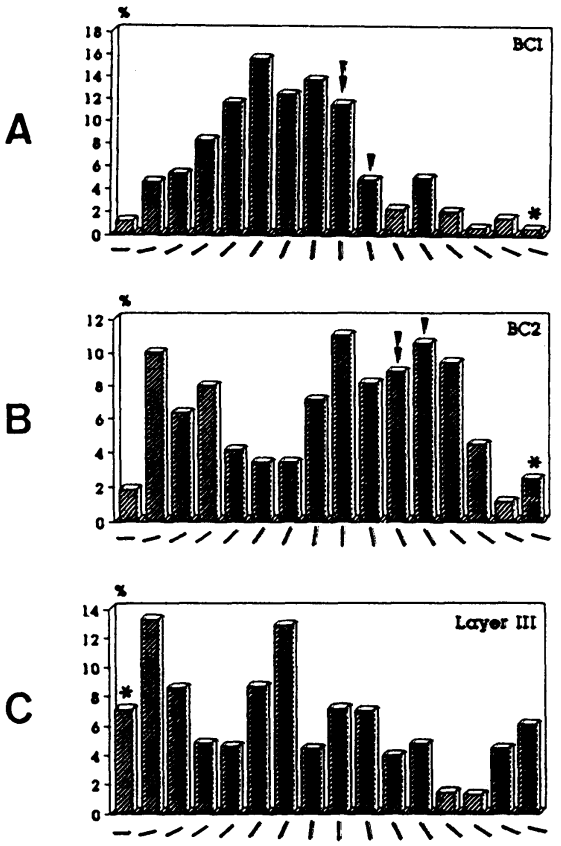

FIG. 7. Frequency distribution of terminals provided by basket cells BC1 (A) and BC2 (B) in layer III at orientation sites indicated by small bars on the abscissa. Double arrowheads mark the average sum of orientation preferences at the soma and the dendritic field (see details in Materials and methods). Single arrowheads show the preferred orientation only at the soma. (C) Frequency distribution of terminals of eight basket cell axons reconstructed in layer III (also shown in Fig. 5). In A–C, asterisks indicate the preferred orientation at the injection site.

tion sites, and only a small minority (3%) entered cross-orientation sites. In part this finding can be explained by the fact that dendritic fields are less widespread than axonal fields although they occasionally extend up to a lateral distance of 300 μm from the parent soma (Fig. 3A).

Discussion

Significance of lateral inhibitory connections

Although pyramidal cells have been generally thought to be the chief source of long-range lateral connections, recent anatomical studies using a combination of retrograde labelling and immunochemistry for GABA showed that ~15% of labelled somata found in remote patches were double-labelled (Albus *et al.*, 1991). In another study, the soma and dendritic morphology of laterally projecting cells was revealed by intracellular labelling (Thejomayen and Matsubara, 1993). Of 109 cells, 15 were non-pyramidal cells whose morphology resembled identified basket cells. From these findings it follows that basket cells constitute a subset in the system of lateral connections, suggesting that their influence, in comparison with the pyramidal system, is weak. It is, however, the fine anatomy of basket cells that indicates a much stronger significance of basket cells than can be anticipated from the above findings. We calculated[1] that each basket cell and each pyramidal cell with patchy axon contacts about equal numbers of other neurons. Importantly, however, a basket cell provides 2–3 times more contacts onto the same target cell than a pyramidal cell. Hence considering the difference in the number of contacts per cell, together with the notion that boutons of basket cells contact the perisomatic region of the target cells, a very influential location from a functional point of view, the two long-range systems might be much more competitive than previously thought.

Overall topography of lateral inhibition

In a recent report based on bouton counts of labelled large basket cells at physiologically characterized sites the proportion of the terminals directed to iso-, oblique- and cross-orientation sites was found roughly equal (Kisvárday and Eysel, 1993). Here we conducted a more accurate assessment of the functional topography of large basket cells using high-resolution orientation maps. The results showed that ~40% of the terminals innervated regions whose orientation preferences differed by less than ±30° from that of the basket cell's own orientation preference. In addition a total of 60% of terminals targeted regions including oblique- and cross-orientation preferences. Given that there is already strong evidence that large basket cells terminate at the perisomatic region of their target neurons, a direct functional correlation between the location of the boutons and the orientation preference of the target cells can be drawn. At this point it is relevant to note that the orientation ranges for distinguishing iso-, oblique- and cross-orientation are artificial categories; under physiological conditions a ±30° offset from the cell's preferred orientation in most cases represents an already non-optimal orientation. Keeping this in mind, the present results provide clear evidence that in the visual cortex of the cat there is a GABAergic cell type, the large basket cell, whose anatomical constraints are well suited to mediate, in addition to iso-orientation inhibition, a substantial amount of non-iso-orientation inhibition, including cross-orientation inhibition in the strictest sense. This conclusion is very much in line with a number of results obtained by extracellular experiments (Sillito, 1975, 1979; Morrone *et al.*, 1982; Ramoa *et al.*, 1986; Eysel *et al.*, 1990), and has common ground with some intracellular studies demonstrating broad-band inhibitory postsynaptic potentials (Benevento *et al.*, 1972; Douglas *et al.*, 1991; Volgushev *et al.*, 1993; but see Ferster, 1986; Ferster and Jagadeesh, 1992).

The relative impact of lateral inhibition along the orientation map

Orientation selectivity has long been known to be regularly distributed along the plane parallel with the cortical surface (Hubel and Wiesel, 1962); a tangential electrode penetration would detect a gradual shift in orientation selectivity, clockwise or counter-clockwise, with a full cycle over ~1–1.5 mm—a hypercolumn—in area 18. Recent work using mapping of orientation preferences, either with multiple electrode penetrations (Cynader *et al.*, 1987) or optical imaging

[1]We estimated the average number of terminals provided by single pyramidal and single large basket cells in layer III. We counted the number of terminals of two intracellularly filled pyramidal cells (Figs 2C and 5B of Gilbert and Wiesel, 1983) and found that each cell emitted an average of 1296 terminals. Bouton counts for layer III large basket cells were taken from this and previous studies (Kisvárday and Eysel, 1993; Kisvárday *et al.*, 1993). Based on six extracellularly labelled cells, an average of 2528 boutons per basket cell was found. Because a pyramidal cell and a basket cell provide 1–4 (Kisvárday and Eysel, 1993) and 5–8 (Somogyi *et al.*, 1983) contacts onto a target cell respectively, it is concluded that both cell types establish input onto a total of 300–600 target neurons.

(Bonhoeffer and Grinvald, 1991), revealed a highly organized distribution of orientation domains or patches along the cortical surface. It is an in intrinsic property of these orientation maps that with increasing lateral distance around any given location in the map the relative occurrence of orientation preferences gradually changes. It is thus relevant to ask here whether the statistics of lateral inhibitory connections to different orientation sites shows parallel changes with increasing distance from their origin (soma location, injection site). Obviously the axons of large basket cells meet this requirement of orientation preferences (frequency of occurrence) along their course. In order to translate the termination pattern of basket cells to a functional interpretation of the data we calculated the 'relative inhibitory impact' of terminals with respect to distance from the cell body and, in the case of the pooled axons, the injection site in the centre (see Materials and methods). The results shown in Figure 8 reveal that iso-orientation inhibition had a strong impact up to a lateral distance of 400 μm and, occasionally, at a hypercolumn distance of 800–1200 μm from the parent soma. Cross-orientation inhibition consistently reached its maximum at half a hypercolumn distance at ~400–800 μm. Oblique-orientation inhibition was reasonably strong over a broad range.

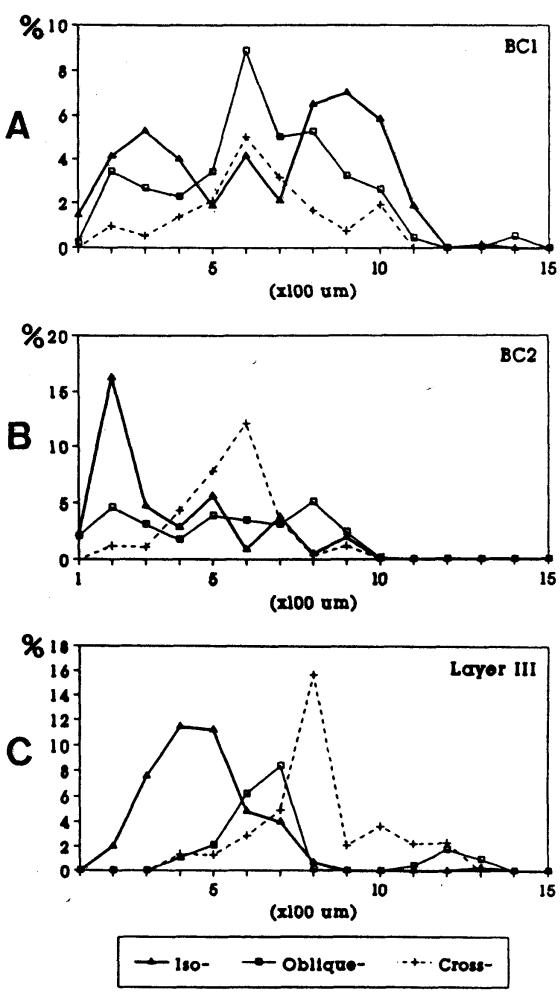

FIG. 8. The impact of lateral inhibitory connections mediated by large basket cells BC1 (in A), BC2 (in B), and eight axons pooled in layer III (in C). Note that iso-orientation inhibition plays a dominant role up to a distance of 400 μm from the parent soma (injection site) and to a lesser extent at a distance of 800–1200 μm. In turn, cross-orientation inhibition is most powerful at a lateral distance of 400–800 μm, and oblique-orientation is reasonably strong in a broad region.

Functional implications

The functional topography of large basket cells within the orientation map raises the question of their possible functional role with respect to orientation and direction selectivity. In order to address this issue the data reported here need to be viewed in the context of recent studies examining the significance of lateral interactions. Matsubara *et al.* (1987) revealed long-range lateral connections with bulk injection of tracers in an area that had been mapped with microelectrodes for orientation preferences. The results showed that the labelled patches were in regions where orientation preferences were orthogonal to that of the injection site. One possible interpretation of the results was that the underlying cross-orientational connections were provided, at least partly, by large basket cells. Our own results support such a view, although the termination pattern of large basket cells, as shown here, is clearly not restricted only to cross-orientation sites. In another study, the contribution of lateral inhibition was directly tested between cortical columns of known orientation preferences separated by some 600 μm from each other (Crook and Eysel, 1992). It was demonstrated that iontophoretic administration of GABA reversibly broadened or in some cases abolished orientation tuning of cells recorded at a remote site whose orientation preference was orthogonal to that of the inactivation site.

Further information on the possible effect of long-range inhibitory connections was obtained in our preliminary study, using the inactivation paradigm in combination with anatomical demonstration of the underlying GABAergic pathway (Crook *et al.*, 1992). There are two important findings to be mentioned. Firstly, when the inactivation and the recording sites had similar orientation preferences the effect was mainly on the directional domain of the recorded cell in a predictable manner. Secondly, GABAergic neurons, many of which had a large soma size, similar to identified large basket cells, were found to project between the recording and the inactivation sites irrespective of their orientation preferences.

Without doubt, the general outcome of the present data is that lateral inhibition is not tuned for either orientation. Thus we are left with seemingly contradictory data, highly specific orientation tuning of most cortical cells and an inhibitory network that is *not specific* for orientation. Part of this paradox was addressed in a recent modelling study by Wörgötter *et al.*, (1991). In their simulation work a non-specific and isotropic inhibitory mechanism, so-called 'circular inhibition', was introduced where inhibitory neurons were arranged in a ring at about half a hypercolumn distance from the target cells, which accounted for heightened orientation selectivity. This model is attractive in that even low structural specificity can elicit functionally specific responses. It is also supported by our statistical analysis of functional impact, where we find an elevated cross-orientation impact at distances postulated for the formation of circular inhibition. Nonetheless, it by no means reflects the real situation in the cortex. For example, our single-cell and population data on basket axons showed that lateral inhibition is not circularly organized, instead only certain directions (sectors) in the visual representation of the cortex are influenced, at least by the long-range inhibitory system, from any given point (Figs 4 and 5). On the other hand, orientation tuning of cortical cells initially might be set up by the geometrical alignment of incoming thalamocortical fibres as originally suggested by Hubel and Wiesel (1962). This model has recently gained support from experiments in which the activity of thalamocortical input was detected in the absence of activity of local cortical neurons (Chapman

et al., 1991). The results showed that in a single penetration the sum of receptive fields of geniculocortical axons generally paralleled the preferred orientation of cortical cells that had been silenced at the same location. All these results suggest that orientation selectivity is most probably brought about by more than one mechanism: an ordered thalamocortical input roughly tunes the target cells for orientation and local inhibitory interactions simultaneously reshape the tuning of these cells to be orientation selective. To achieve this the inhibitory input ought to derive from sites whose orientation preference is predominantly different from that of the targeted region. The present study shows that such a task might be well suited to large basket cells.

Conclusion

The central question whether lateral inhibition is specifically tuned for any particular orientation was tested. The data of this study confirmed our previous results and showed that long-range lateral inhibitory connections supplied by large basket cells established monosynaptic pathways between sites of many orientations, as schematically shown in the upper panel of Figure 9. In addition, the present results prove that the terminal fields of individual basket axons displayed an ordered distribution along the plane of the orientation map, predominantly iso-orientation inhibition close to their origin and predominantly non-iso-orientation inhibition more remotely. No obvious clustering of basket cell terminals according to the orientation domains was seen. The populations of basket axons originating from a narrow column of cells in layer III behaved similarly to the single cells.

On the basis of the present findings and those of our previous study (Kisvárday and Eysel, 1993), the simplest implication of the functional topography of large basket cells is that they simultaneously mediate orientation inhibition and direction inhibition, maybe to the same target cell, in a balanced manner. This assumption is illustrated in the lower panel of Figure 9, in which a vertical line projected from the position of a target cell in the upper panel intersects the two curves in the lower panel and delineates the relative effects of the basket cell on direction (arrowed field) and orientation (stippled field) selectivity onto its target cell. It is conceivable that the relative effects on direction and orientation selectivity gradually change with distance from the basket cell; importantly, with emphasis on orientation inhibition at sites of dissimilar orientation and with emphasis on direction inhibition at sites of similar orientation with respect to the basket cell's own orientation preference. Although one might argue that there is no *a priori* reason to assign orientation and direction selectivity as part of the functional duty of large basket cells, the weight of evidence (this study; Kisvárday *et al.*, 1993; for details see Kisvárday and Eysel, 1993) favours this view. Inevitably, the acid test on this matter, e.g. simultaneous recording from a large basket cell and one of its target neurons, awaits future studies.

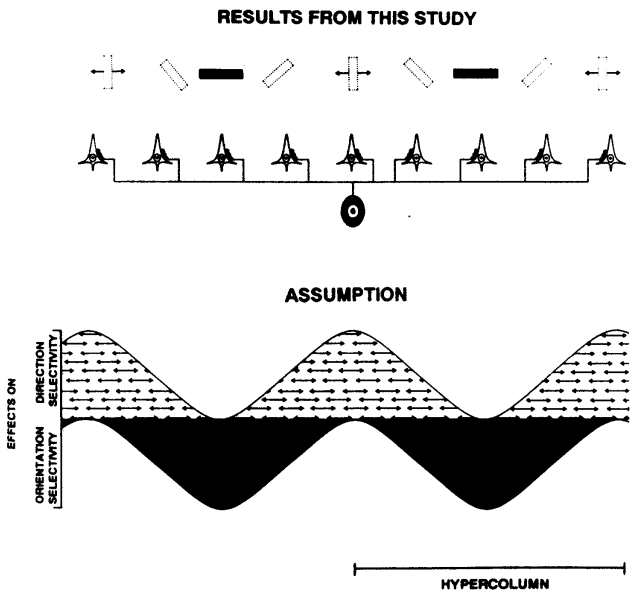

FIG. 9. Upper diagram shows the topographical arrangement of large basket cell connections according to orientation selectivity. The basket cell is indicated by a black oval symbol and the target cells are pyramid-shaped. Orientation preferences are shown by bars at the top of the panel. Lower diagram shows the possible functional implication of the above topography (see further details in the text).

Acknowledgements

The authors thank Eva Tóth and Frank Brinkmann for their excellent technical assistance, and Dorothy Strehler for high-quality photography. We are grateful to Ferenc Leeb for writing the program for bouton counts and Wolf Singer for his support. Z. F. K. was supported by the Alexander von Humboldt Foundation and the Deutsche Forschungsgemeinschaft, T. B. was in part supported by a Helmholtz Stipend from the Bundesministerium für Forschung und Technologie. This work was supported by the Deutsche Forschungsgemeinschaft (Ey8/17-1 to U. T. E.) and the European Communities (SC1 0329-C to U. T. E.).

Abbreviations

ECG	electrocardiogram
EEG	electroencephalogram
PB	phosphate buffer

References

Albus, K. (1975) A quantitative study of the projection area of the central and the paracentral visual field in area 17 of the cat. II The spatial organization of the orientation domain. *Exp. Brain Res.*, **24**, 181–202.

Albus, K., Wahle, P., Lübke, J. and Matute, C. (1991) The contribution of GABA-ergic neurons to horizontal intrinsic connections in upper layers of the cat's striate cortex. *Exp. Brain Res.*, **85**, 235–239.

Benevento, L. A., Creutzfeldt, O. D. and Kuhnt, U. (1972) Significance of intracortical inhibition in the visual cortex. *Nature*, **238**, 124–126.

Blakemore, C. and Tobin, E. A. (1972) Lateral inhibition between orientation detectors in the cat's visual cortex. *Exp. Brain Res.*, **15**, 439–440.

Blasdel, G. G. and Salama, G. (1986) Voltage-sensitive dyes reveal a modular organization in monkey striate cortex. *Nature*, **321**, 579–585.

Bonhoeffer, T. and Grinvald, A. (1991) Iso-orientation domains in cat visual cortex are arranged in pinwheel-like patterns. *Nature*, **353**, 429–431.

Bonhoeffer, T. and Grinvald, A. (1993) The layout of iso-orientation domains in area 18 of cat visual cortex. Optical imaging reveals pinwheel-like organization. *J. Neurosci.*, **13**, 4157–4180.

Chapman, B., Zahs, K. R. and Stryker, M. P. (1991) Relation of cortical cell orientation selectivity to alignment of receptive fields of the geniculocortical afferents that arborize within a single orientation column in ferret visual cortex. *J. Neurosci.*, **11**, 1347–1358.

Creutzfeldt, O. D., Kuhnt, U. and Benevento, L. A. (1974) An intracellular analysis of visual cortical neurones to moving stimuli: Responses in a cooperative neuronal network. *Exp. Brain Res.*, **21**, 251–274.

Crook, J. M. and Eysel, U. T. (1992) GABA-induced inactivation of functionally characterized sites in cat visual cortex (area 18): effects on orientation tuning. *J. Neurosci.*, **12**, 1816–1825.

Crook, J. M., Kisvárday, Z. F. and Eysel, U. T. (1992) Contribution of lateral inhibition to orientation and direction selectivity in cat visual cortex (area

18): GABA-inactivation combined with injections of [^{3}H]-nipecotic acid. In Elsner, N. and Richter, D. (eds), *Rhythmogenesis in Neurons and Networks. Proceedings of the 20th Göttingen Neurobiology Conference*, p. 355.

Cynader, M. S., Swindale, N. V. and Matsubara, J. A. (1987) Functional topography in cat area 18. *J. Neurosci.*, **7**, 1401–1413.

Douglas, R. J., Martin, K. A. C. and Whitteridge, D. (1991) An intracellular analysis of the visual responses of neurones in cat visual cortex. *J. Physiol. (Lond.)*, **440**, 659–696.

Eysel, U. T., Muche, T. and Wörgötter, F. (1988) Lateral interactions at direction selective striate neurones in the cat demonstrated by local cortical inactivation. *J. Physiol. (Lond.)*, **399**, 657–675.

Eysel, U. T., Crook, J. M. and Machemer, H. F. (1990) GABA-induced remote inactivation reveals cross-orientation inhibition in the striate cortex. *Exp. Brain Res.*, **80**, 626–630.

Ferster, D. (1986) Orientation selectivity of synaptic potentials in neurons of cat primary visual cortex. *J. Neurosci.*, **6**, 1284–1301.

Ferster, D. and Jagadeesh, B. (1992) EPSP–IPSP interactions in cat visual cortex studied with *in vivo* whole-cell patch recording. *J. Neurosci.*, **12**, 1262–1274.

Frostig, R. D., Lieke, E. E., T'so, D. Y. and Grinvald, A. (1990) Cortical functional architecture and local coupling between neuronal activity and the microcirculation revealed by *in vivo* high-resolution optical imaging of intrinsic signals. *Proc. Natl Acad. Sci. USA*, **87**, 6082–6086.

Gilbert, C. D. and Wiesel, T. N. (1983) Clustered intrinsic connections in cat visual cortex. *J. Neurosci.*, **3**, 1116–1133.

Henry, G. H., Dreher, B. and Bishop, P. O. (1974) Orientation specificity of cells in cat striate cortex. *J. Neurophysiol.*, **37**, 1394–1409.

Hubel, D. H. and Wiesel, T. N. (1962) Receptive fields, binocular interaction and functional architecture in the cat's visual cortex. *J. Physiol. (Lond.)*, **160**, 106–154.

Hubel, D. H. and Wiesel, T. N. (1963) Shape and arrangement of columns in cat's striate cortex. *J. Physiol. (Lond.)*, **165**, 559–568.

Hubel, D. H. and Wiesel, T. N. (1965) Receptive fields and functional architecture in two nonstriate visual areas (areas 18 and 19) of the cat. *J. Neurophysiol.*, **28**, 229–289.

Kisvárday, Z. F. (1992) GABAergic networks of basket cells in the visual cortex. In Mize, R. R., Marc, R. and Sillito, A. M. (eds), *Progress in Brain Res, Vol. 90, Mechanisms of GABA in the Visual System*. Elsevier, Amsterdam, pp. 385–405.

Kisvárday, Z. F. and Eysel, U. T. (1993) Functional and structural topography of horizontal inhibitory connections in cat visual cortex. *Eur. J. Neurosci.*, **5**, 1558–1572.

Kisvárday, Z. F., Kim, D.-S., Eysel, U. T. and Bonhoeffer, T. (1992) Functional and structural topography of lateral inhibitory connections in cat visual cortex (area 18). *Soc. Neurosci.*, **18**, 388.

Kisvárday, Z. F., Beaulieu, C. and Eysel, U. T. (1993) Network of GABAergic large basket cells in cat visual cortex (area 18). Implications for lateral disinhibition. *J. Comp. Neurol.*, **327**, 398–415.

Matsubara, J. A., Cynader, M. S. and Swindale, N. V. (1987) Anatomical properties and physiological correlates of the intrinsic connections in cat area 18. *J. Neurosci.*, **7**, 1428–1446.

Morrone, M., Burr, D. C. and Maffei, L. (1982) Functional implications of cross-orientation inhibition of cortical visual cells. I. Neurophysiological evidence. *Proc. R. Soc. Lond. B*, **216**, 335–354.

Ramoa, A. S., Shadlen, M., Skottun, B. C. and Freeman, R. D. (1986) A comparison of inhibition in orientation and spatial frequency selectivity of cat visual cortex. *Nature*, **321**, 237–239.

Sillito, A. M. (1975) The contribution of inhibitory mechanisms to the receptive field properties of neurones in the striate cortex of the cat. *J. Physiol. (Lond.)*, **250**, 305–329.

Sillito, A. M. (1977) Inhibitory processes underlying the directional specificity of simple, complex and hypercomplex cells in the cat's visual cortex. *J. Physiol. (Lond.)*, **271**, 699–720.

Sillito, A. M. (1979) Inhibitory mechanisms influencing complex cell orientation selectivity and their modification at high resting discharge levels. *J. Physiol. (Lond.)*, **289**, 33–53.

Somogyi, P., Kisvárday, Z. F., Martin, K. A. C. and Whitteridge, D. (1983) Synaptic connections of morphologically identified and physiologically characterized large basket cells in the striate cortex of cat. *Neuroscience*, **10**, 261–294.

Thejomayen, D. M. and Matsubara, J. A. (1993) Confocal microscopic study of the dendritic organization of patchy, intrinsic neurons in area 18 of the cat. *Cerebral Cortex*, **3**, 442–453.

T'so, D. Y., Frostig, R. D., Lieke, E. E. and Grinvald, A. (1990) Functional organization of primate visual cortex revealed by high resolution optical imaging. *Science*, **249**, 417–420.

Tsumoto, T., Eckart, W. and Creutzfeldt, O. D. (1979) Modification of orientation sensitivity of cat visual cortex neurons by removal of GABA-mediated inhibition. *Exp. Brain Res.*, **34**, 351–363.

Volgushev, M., Pei, X., Vidyasagar, T. R. and Creutzfeldt, O. D. (1993) Excitation and inhibition in cortical orientation selectivity revealed by whole cell recordings *in vivo*. *Vis. Neurosci.*, **10**, 1151–1155.

Wörgötter, F., Niebur, E. and Koch, C. (1991) Isotropic connections generate functional asymmetrical behaviour in visual cortical cells. *J. Neurophysiol.*, **66**, 444–459.